

# Zero-tuning Grinding Process Methodology of Cyber-Physical Robot System

Hsuan-Yu Yang<sup>1,3</sup>, Chih-Hsuan Shih<sup>2,3</sup>, Yuan-Chieh Lo<sup>3</sup> and Feng-Li Lian<sup>1,3</sup>, *Senior Member, IEEE*

**Abstract**—Industrial robots play potential and important roles on labor-intensive and high-risk jobs. For example, typical industrial robots have been used in grinding process. However, the automatic grinding process by robots is a complex process because it still relies on skillful engineers to adaptively adjust several key parameters. Moreover, it might take a lot of time and effort to yield better grinding quality. Hence, this paper proposed a new framework of cyber-physical robot system with automatic zero-tuning optimization of the process parameters to achieve the desired quality. To overcome the unexpected difference between reality and simulation, proper system calibration can help in precise positioning in real environment, and the cloud database is constructed to record the relative data during the grinding process simultaneously. The proposed zero-tuning methodology combines both neural network (NN) model and genetic algorithm (GA) to generate the best combination of corresponding parameters to meet the desired quality. Experimental results showed that the average error of the output result was 8.93%. To compare the CNC machine, our solution shows more prominent role and potential in plumbing industry.

## I. INTRODUCTION

INDUSTRIAL robots have been widely used in many manufacturing and machining processes, such as cargo handling, welding, spraying, etc. [1]. Moreover, industrial robots are also applied in labor-intensive and high-risk industries, such as in plumbing industry, which traditionally relies on labors to manually grind and polish the workpieces. However, the operating environment is filled with noise and the grinding process also causes serious industrial dust pollution that is detrimental to health. These drawbacks result in a high turnover rate, and the factories are often faced with severe problem of labor shortage. Although industrial robots can replace human to accomplish the works, the ultimate solution still depends on experienced or skillful engineer to fine-tune the related process parameters for better grinding quality. Hence, current grinding processes are not fully automated.

The combination of different process parameters can affect the grinding quality by robotic system [2], such as the belt grain size, the robot moving speed, the belt machine line speed and the grinding contact force, etc. [3]. When different combinations of process parameters are used, it will lead to different quality of the workpiece, including the difference in

surface roughness, residual of casting surface, mismatch gap and surface discontinuity.

Traditional methods to predicting the surface roughness and optimized process parameters would involve a construction of physical grinding model. For example, Zhang et al. [4] proposed a pressure distribution model combined with other grinding parameters to estimate the material removal of robotic grinding. Wu et al. [5] constructed a platform for comprehensive modeling and simulation of the robotic belt grinding system to select the grinding process key parameters. Zhao et al. [6] established a surface roughness prediction model for CNC belt grinding and polishing machine, and the optimum process parameters were determined by analyzing the response surface to improve surface quality and reduce surface roughness of integrally bladed rotors. Ng et al. [7], [8] scaled the manual grinding parameters to robotic grinding platform by building a depth pixel model and a material removal model. Qi and Chen [3] designed a prediction model based on the average cutting depth of abrasive grains to predict the surface roughness for robotic grinding, where the grinding belt was fixed on the robot. Zhu et al. [9] built a surface roughness prediction model to predict the surface roughness of SiCp/Al composite using the surface grinder and optimized the grinding process parameters by Non-dominant Sorting Genetic Algorithm (NSGA-II).

However, robotic grinding is a complex process that is difficult to match fully the real environment with fitting parameters in a model that can fully reflect the system. To solve the problem of comprehensive parameter optimization, a potential solution may depend on machine learning associated with Big Data [10], which is already widely used to predict the surface roughness in hard turning [11]. Therefore, this paper proposed a neural network model combined with genetic algorithm to construct a “zero-tuning” system that can predict the workpiece quality of robotic grinding and automatically tune the process parameters to achieve the desired surface roughness to solve the dependency of human trial and error in tuning.

The rest of the paper is organized as follows. Section II describes the system structure. Section III explains the relative theories and methods. Section IV shows the experimental results. Section V gives conclusions and summarizes this paper.

<sup>1</sup>Department of Electrical Engineering, National Taiwan University, Taipei, 10617, Taiwan. (email: r07921006@ntu.edu.tw)

<sup>2</sup>Department of Computer Science and Information Engineering, National Taiwan University, Taipei, 10617, Taiwan.

<sup>3</sup>Mechanical and Mechatronics System Research Laboratories, Industrial Technology Research Institute, Hsinchu, 31040, Taiwan.

## II. SYSTEM STRUCTURE

### A. Overview of the Robot Grinding Cell

The experimental hardware setup, shown in Figure 1, consisted of an Evermore RH60 robot, an Evermore grinding machine, a dust collector, a Wacoh 6-axis F/T sensor Dynpick 1000 N, a Mitutoyo SJ-210 surface roughness tester and HCG brass faucets (product type: 3188). An Evermore six-axis industrial robot RH60 with payload of 60Kg was used with ITRI robot controller. A Wacoh 6-axis F/T sensor Dynpick 1000 N was installed onto the robot's end-effector to measure the force and torque values during grinding. A Mitutoyo SJ-210 surface roughness tester would measure the surface roughness of the workpiece before and after grinding. A network hub was the central connection for all devices, in which, the cloud-database system could monitor all sensors' signals and the robot information simultaneously.

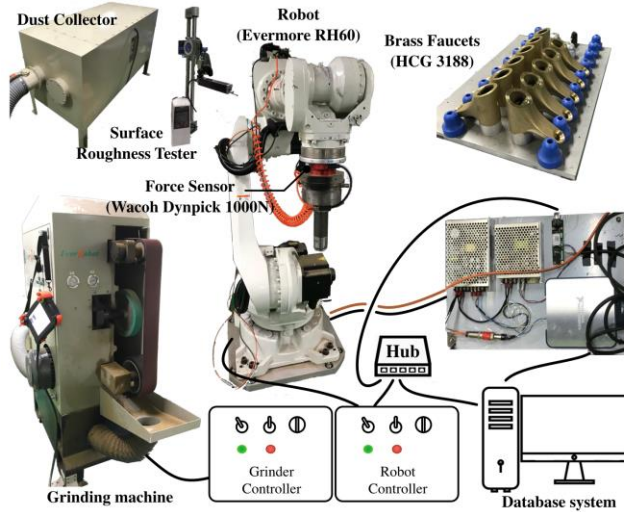


Figure 1. Hardware setup of intelligent robot grinding system in ITRI laboratory.

### B. System Architecture

The comprehensive name of the system architecture of the intelligent robot grinding is described as a cloud-cyber-physical system, as shown in Figure 2.

First, the physical layer deals with sensors, actuators, robots and grinding-related device. One of the critical problems in the robot grinding system is to determine the proper position for the grinding machine in relation to other apparatus, which directly affects the performance of the system. Moreover, the designs of gripper and the grinding machine with proper selection of the abrasive belt are important as well.

Second, the cyber layer is established based on the robot's programming software, EzSim, which is developed by ITRI robotics team. The EzSim Software Developed Kit (SDK) supports users with functional APIs for developing various kinds of application technology. To eliminate the error between physical model and cyber model, the calibration process plays an important role. Thus, one smart vision plugin

is developed for this purpose. Additionally, the status plugin monitors and records not only the sensor signal, the robot joint value, and Cartesian pose, but also the ideal trajectory planned in offline programming, to be stored as one dataset in JSON structure for each grinding process. Moreover, the zero-tuning methodology can access those grinding datasets from cloud database. With appropriate query method, it retrieves meaningful data as training and validating sets for further machine learning purpose.

Lastly, the cloud layer is established based on MongoDB [12]. Since it is highly possible that the hardware installation of every robot grinding system varies, therefore, NoSQL database has the advantage of flexible and schema-free structure applicable in this circumstance.

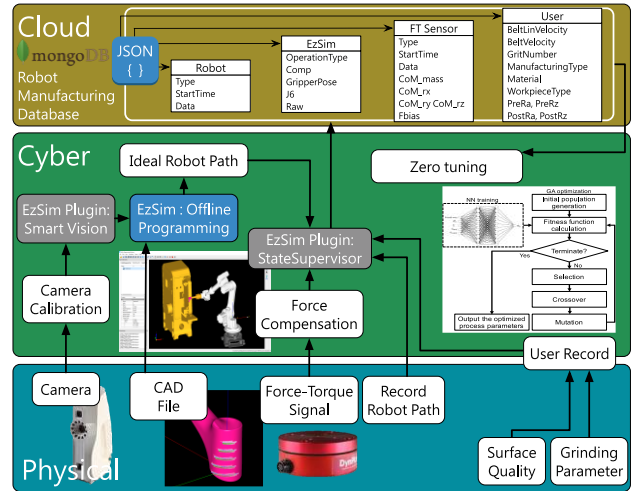


Figure 2. System architecture of cyber-physical-cloud manufacturing system.

## III. RELATED THEORIES AND METHODS

### A. System Calibration

To synchronize the data and information between physical shop floor and the cyber computational space, the system calibration plays an important role in cyber-physical robotic system. Furthermore, the database relies on well-defined configuration to collect useful information. This research focused on the grinding process and tried to find the relationship between process parameters and surface quality of workpieces, in which the position of the belt grinding machine and its contact force are two important factors to affect the final quality. However, the measuring signal from F/T sensor involves many elements, such as sensor bias, gravity, vibration, inertial force and noise, being expressed as follows:

$$F_{sensor} = F_{bias} + F_{gravity} + F_{vibration} + F_{contact} + F_{noise} \quad (1)$$

Bias and gravity compensation are the essential steps for measuring the contact force by F/T sensor [13], and their experimental results are listed in Table 1.

Table 1. The experiment results of bias and gravity compensation

Parameters	Values
Mass (kg)	12.38
Center of mass (mm)	(0.11, 0.63, 113.16)

The other important factor in grinding process is to calibrate the position and orientation of the belt grinding machine beforehand. It can help eliminate the difference between reality and simulation with immediate refining of the trajectory of robot to reduce complex procedure of tuning. This research adopts a scheme of using a sensory 3D camera as eye-in-hand configuration to positioning and orientation of grinding machine. The main advantage of this sensory scheme is its range of detection, providing the maximum sensory capability. Before locating the grinding machine, the rigid transformation between the camera frame and the robot end-effector must be computed in advance and such issue was already formulated by our previous work [14].

### B. Robot Trajectory Generation

In order to generate a more accurate robot trajectory when using simulation, this paper developed the simulator equipped with CAD/CAM engine to automatically generate the toolpath of workpiece. The principal of toolpath generation in the simulator is based on the iso-planar method [15]. First, the CAD model of workpiece must be loaded into the simulator. Then, the workpiece features such as vertex, edge and surface are extracted by operator to select specific area. The toolpaths are generated by intersecting surface in Cartesian space and characterized with a uniform interval between adjacent toolpaths. After that, the robot trajectory must be transformed by toolpath of workpiece that is composed of a position vector and its normal vector. However, the difference between reality and simulation often leads to uncertainty, and to counter this problem of uncertainty, a machine localization approach for calibrating the grinding machine position precisely was proposed. Following the calibration results of machine location, the robot trajectory can be modified and optimized in real-time. Figure 3 shows the transformation of the robotic belt grinding system. The problem can be formulated as follows:

$${}^R H_G = {}^R H_B {}^B H_G = {}^R H_E {}^C H_E^{-1} {}^C H_B {}^B H_G \quad (2)$$

where  ${}^R H_G \in R^{4 \times 4}$  represents rigid transformation between the robot base and grinding contact point.  ${}^B H_G \in R^{4 \times 4}$  represents rigid transformation between grinding machine and grinding contact point, which can be determined by the simulation setting.  ${}^R H_B \in R^{4 \times 4}$  represents rigid transformation between robot base and grinding machine. It was hard to yield an ideal match between simulated and real distance. Therefore, a 3D camera was used to calibrate the grinding machine's position, and the ICP algorithm was applied to find the relationship between the CAD model of grinding machine and camera sensing data [16]. This information can be calculated by following

transformations.  ${}^R H_E \in R^{4 \times 4}$  represents rigid transformation between the robot end-effector and the robot base.  ${}^C H_E = X \in R^{4 \times 4}$  represents rigid transformation between the camera frame and the robot end-effector.  ${}^C H_B \in R^{4 \times 4}$  represents rigid transformation between the camera frame and the grinding machine.

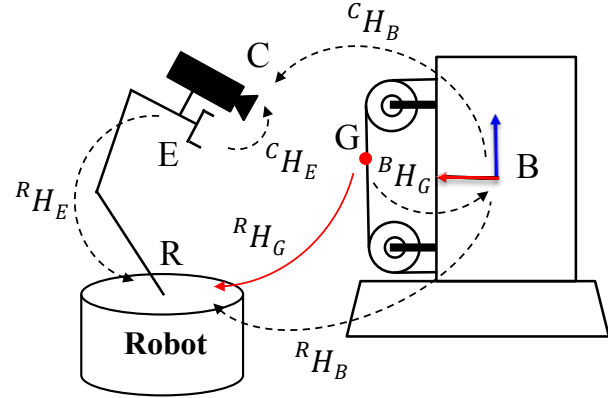


Figure 3. Transformation of the robotic belt grinding system.

### C. Surface Roughness Estimation

The grinding surface quality is affected by the combination of different process parameters such as the belt grain size, the belt machine line speed, and workpiece material, etc. In this research, a neural network technique (NN) was employed for predicting the surface roughness during robotic grinding process. To establish the modeling of the surface roughness, a popular, three-tier layer architecture of feedforward neural network was used based on the back-propagation learning algorithm. The numbers of neuron in the input, the hidden, and the output layers were five, ten, ten and one, respectively, as shown in Figure 4. The input neurons were respectively monitoring the belt grain size, the surface roughness before grinding, the belt machine line speed, the robot arm velocity and the contact force. The output of the model was the surface roughness after grinding. The NN performances were evaluated using mean absolute error (MAE) which is expressed in Eq. (3):

$$MAE = \frac{1}{n} \sum_{i=1}^n | {}^i R_a - {}^i \tilde{R}_a | \quad (3)$$

where  ${}^i R_a$  is the predicted surface roughness after grinding generated by NN,  ${}^i \tilde{R}_a$  is the actual surface roughness after grinding measured by the surface roughness tester and  $n$  is the size of sample data.

### D. Grinding Process Parameters Optimization

The neural network can be used to construct the complicated relationship between grinding parameters and surface roughness. In order to achieve the desired quality, one genetic algorithm was used to optimize the grinding parameters as the inputs of the NN model, which included the belt grain size, the surface roughness value before grinding  $R'_a$ , the contact force  $f_c$ , the belt line speed  $v_{belt}$  and the robot

velocity  $v_{robot}$ . The output of the NN model was the surface roughness value after grinding  $R_a$ . The fitness function of genetic algorithm was the training result of NN model. Afterwards, the genetic algorithm was repeated for selection, crossover, and mutation to create the new population that could satisfy the requirements of the fitness function, as shown in Figure 5. Eventually, the output of the genetic algorithm is the optimized combination of process parameters, which is the objective of this zero-tuning system for achieving the desired surface roughness by robotic grinding.

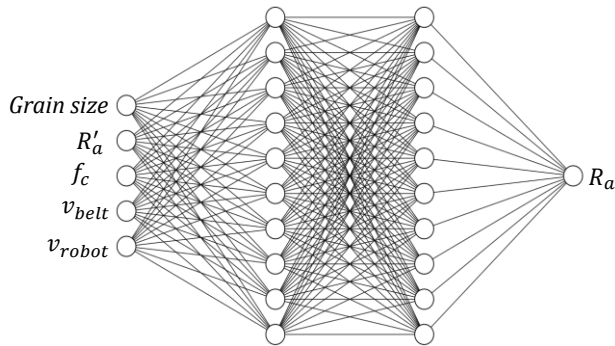


Figure 4. The architecture of 5-10-10-1 neural network.

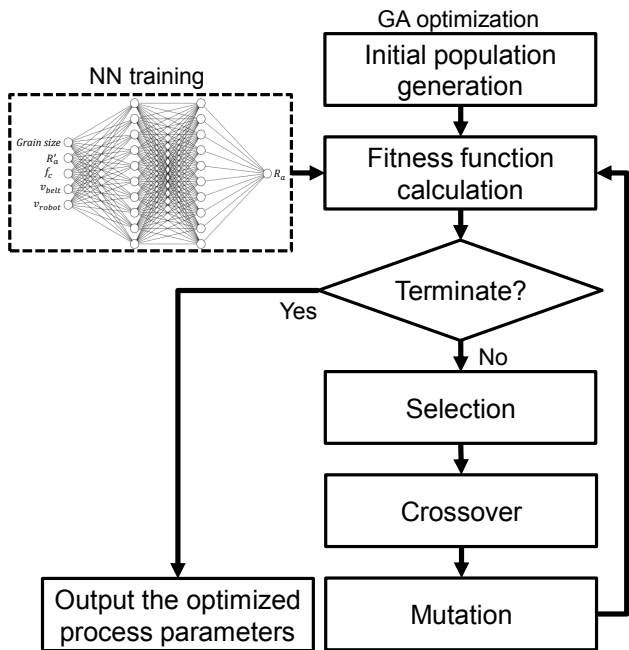


Figure 5. The architecture of zero-tuning system.

#### IV. EXPERIMENT AND ANALYSIS

In the setup of the hand-eye calibration experiment, an Evermore RH60 robot was used with an Artec Eva 3D camera. First, the robot was manipulated to acquire 50 poses and camera images that contained 96 grid chessboards, as shown in Figure 6. In order to receive reliable calibration result, the system implemented three calibration techniques to select the best one to locate the machine position. In addition, the calibration results were validated by the robot hand-eye calibration using calibration image set. The errors of

hand-eye calibration are listed in Table 2.

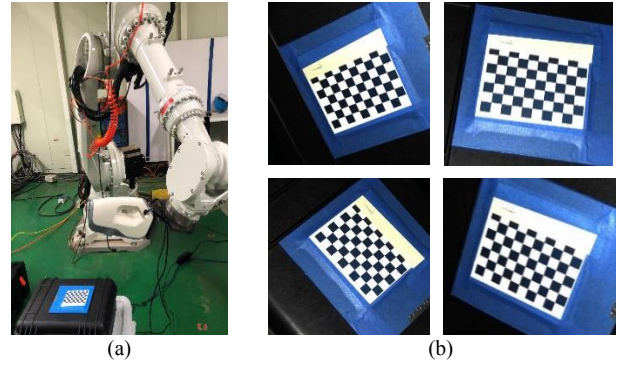


Figure 6. (a) Hand-eye calibration experiment setup. (b) Collection of input images.

Table 2. The transformation errors of the calibration grid points

Methods	Mean (mm)	Std (mm)
Park94 [17]	1.891956	0.856799
Daniilidis98 [18]	1.881985	0.76816
Andreff99 [19]	4.121095	3.194093

To collect the data on robotic grinding, the copper alloy faucet blank was chosen for the experiment as shown in Figure 7. The grinding process parameters are listed in Table 3.

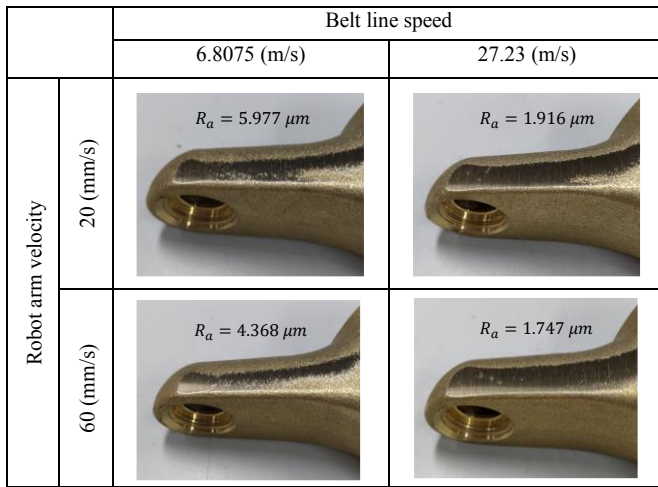


Figure 7. A workpiece of copper alloy faucet blank.

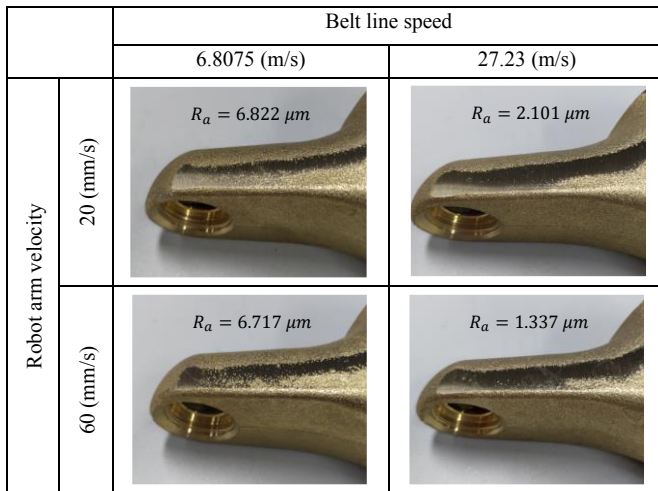
Table 3. Processing parameters of data collection

Parameters	Values
Grid belt	#100. #280. #400
Belt machine line velocity	6.8075. 13.615. 27.23 (m/s)
Robot arm velocity	20. 40. 60 (mm/s)

There are 3 different parameters: the belt grain size, the belt machine line speed and the robot arm velocity. Each parameter has 3 different values. As a result, there will be a total of 27 combinations. For each combination, the grinding procedure was repeated three times, and thus, a total of 81 data pieces have been collected and saved in the proposed cloud robot grinding database system. Figure 8 shows a part of the grinding results under different process parameters. It was observed that different combinations of parameters yielded different surface conditions of the workpiece. For instance, the grinding belt with a slow line velocity resulted in more residues on the casting surface after robotic grinding, compared with a fast belt line speed.



(a) #100



(b) #400

Figure 8. The robotic grinding results under different parameters' combination. (a) The belt grain size of #100 with different belt machine line speed and robot arm velocity. (b) The belt grain size of #400 with different belt machine line speed and robot arm velocity.

The data of the robotic grinding would then be applied to the NN model, which is described in Section III C. The training epoch was 350, with the result shown in Figure 9. The training error and test error were 0.5135 and 0.4141, respectively. Then, the model became the fitness function of the genetic algorithm to find the optimum process parameters for the desired surface roughness by grinding. In genetic algorithm, the population size was set to 50, the crossover rate was set to 0.8, and the mutation rate was set to 0.03. Due to the limitation of robotic grinding system, the process parameters have specific operating ranges during the optimization part in genetic algorithm as shown in Table 4. There are three different kinds of choices for the belt grain size. The belt machine line speed, the robot arm velocity and the contact force were set in a safety range to ensure the stability of robotic grinding.

The experimental results for the zero-tuning system are shown in Table 5. There were four testing workpieces with desired surface roughness after grinding, which were having

values of 1.8, 2.4, 3.0 and 3.6, respectively. The genetic algorithm combined with the NN model could successfully calculate the optimum parameters combination within 10 cycles, and the predicted surface roughness error was less than  $0.01\mu\text{m}$ . For the real surface roughness of the workpiece which was grinded with the optimum combination of these parameters, it was observed that the errors between the desired and real surface roughness were all lower than 14% and two errors of the tests were even lower than 9%. In terms of saving time, it was estimated that more than 90% of the time was saved when contrasting the proposed approach and the manual parameters tuning. The experiment proved that the “zero-tuning” system could successfully optimize the parameters for desired surface roughness by grinding.

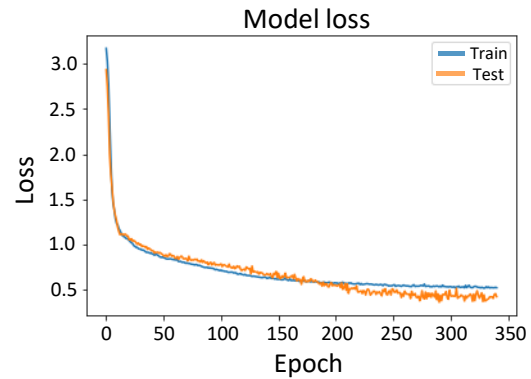


Figure 9. The training result of the neural network model.

Table 4. The range of the processing parameters in robotic grinding system

Parameters	Values
Belt grain size	#100, #280, #400
Belt machine line speed	1.67~27.23 (m/s)
Robot arm velocity	5~100 (mm/s)
Contact Force	5~40 (N)

Table 5. Comparison of the desired, zero-tuning system (ZTS) predicted and real surface roughness after robotic grinding

No.	Desired post Ra ( $\mu\text{m}$ )	ZTS predicted post Ra ( $\mu\text{m}$ )	Real post Ra ( $\mu\text{m}$ )	Error (desired & real)
1	1.8	1.794	1.810	0.56%
2	2.4	2.403	2.709	12.88%
3	3.0	2.990	2.582	13.93%
4	3.6	3.593	3.901	8.36%

To prove the effectiveness of the proposed method, Table 6 shows the results of the comparison. It was observed that the average error of the zero-tuning system was similar to other approaches. Although the three methods all focused on grinding parameters optimization, the scenario of this paper emphasized on robotic grinding, while others involved CNC grinding. Due to the advantages of flexible manufacturing, Single Minute Exchange of Die (SMED) and low price, compared with the CNC machine, industrial robots are more suitable to be applied in the plumbing industry.

Table 6. Comparison between the result in this paper and other references

Method	Average error
This paper	8.93%
[9]	8.78%
[20]	8.43%

## V. CONCLUSION

In this paper, a zero-tuning system that can automatically optimize the process parameters in robotic grinding to match with the desired quality by grinding was presented. First, a cloud-cyber-physical system was developed to accomplish system calibration and robot trajectory prediction, along with an established cloud database in simultaneous recording of the relative data during the grinding process. Next, the zero-tuning system combined with a neural network model and genetic algorithm was designed to generate the most corresponding combination of parameters that could satisfy needs. The results of the experiment showed that the average error of the output result was 8.93%. In comparison with the CNC machine, our solution showed more potential for plumbing industry. Future work involves more data collection to enhance the robustness of the NN model. Other parameters may also be incorporated in the system to improve the prediction rate.

## ACKNOWLEDGMENT

This research is supported by the Ministry of Science and Technology, Taiwan, under Grants: MOST 105-2221-E-002-135-MY3 and MOST 108-2634-F-002-0024, and by Industrial Technology Research Institute, Hsinchu, Taiwan.

## REFERENCES

- [1] S. B. Niku, "Introduction to Robotics: Analysis, Control, Applications," 2nd ed., New York: Wiley, 2010.
- [2] S. N. Grigoriev, V. K. Starkov, N. A. Gorin, P. Krajnik and J. Kopač, "Creep-Feed Grinding: An Overview of Kinematics, Parameters and Effects on Process Efficiency," *Journal of Mechanical Engineering*, vol. 60, Issue 4, pp.213-220, Apr. 2014.
- [3] J. Qi and B. Chen, "Surface Roughness Prediction Based on the Average Cutting Depth of Abrasive Grains in Belt Grinding," in *Proceedings of International Conference on Mechanical, Control and Computer Engineering*, Huhhot, China, Sep. 14-16, 2018.
- [4] X. Zhang, M. Cabaravdic, K. Kneupner and B. Kuhlencoetter, "Real-Time Simulation of Robot Controlled Belt Grinding Processes of Sculptured Surfaces," *International Journal of Advanced Robotic Systems*, vol. 1, No. 2, pp.109-114, Jun. 2004.
- [5] S. Wu, K. Kazerounian, Z. Gan and Y. Sun, "A Simulation Platform for Optimal Selection of Robotic Belt Grinding System Parameters," *International Journal of Advanced Manufacturing Technology*, vol. 64, Issue 1-4, pp.447-458, Jan. 2013.
- [6] T. Zhao, Y. Shi, X. Lin, J. Duan, P. Sun and J. Zhang, "Surface Roughness Prediction and Parameters Optimization in Grinding and Polishing Process for IBR of Aero-engine," *International Journal of Advanced Manufacturing Technology*, vol. 74, Issue 5-8, pp.653-663, Sep. 2014.
- [7] W. X. Ng, H. K. Chan, W. K. Teo and I. M. Chen, "Programming Robotic Tool-Path and Tool-Orientations for Conformance Grinding based on Human Demonstration," in *Proceedings of IEEE/RSJ International Conference on Intelligent Robots and Systems*, Daejeon, Korea, Oct. 9-14, 2016.
- [8] W. X. Ng, H. K. Chan, W. K. Teo and I. M. Chen, "Programming a Robot for Conformance Grinding of Complex Shapes by Capturing the Tacit Knowledge of a Skilled Operator," *IEEE Transactions on*

- Automation Science and Engineering*, vol. 14, No. 2, pp. 1020-1030, Apr. 2017.
- [9] C. Zhu, P. Gu, Y. Wu, D. Liu and X. Wang, "Surface Roughness Prediction Model of SiCp/Al Composite in Grinding," *International Journal of Mechanical Sciences*, vol. 155, pp. 98-109, May 2019.
- [10] W. Ji and L. Wang, "Industrial Robotic Machining: a Review," *International Journal of Advanced Manufacturing Technology*, vol. 103, Issue 1-4, pp. 1239-1255, Jul. 2019.
- [11] K. He, M. Gao and Z. Zhao, "Soft Computing Techniques for Surface Roughness Prediction in Hard Turning: a Literature Review," *IEEE Access*, vol. 7, pp. 89556 - 89569, Jul. 2019.
- [12] K. Chodorow, "MongoDB: The Definitive Guide," 2nd ed., O'Reilly Media, Inc, 2013.
- [13] S. Vougioukas, "Bias Estimation and Gravity Compensation for Force-Torque Sensors," in *Proceedings of International Conference on Mathematical Methods and Computational Techniques in Electrical Engineering*, Athens, Greece, Dec. 29-31, 2001.
- [14] C. H. Shih and F. L. Lian, "Grinding Complex Workpiece Surface Based on Cyber-Physical Robotic Systems," in *Proceedings of IEEE International Conference on Industrial Cyber Physical Systems*, Taipei, Taiwan, May 6-9, 2019.
- [15] H. Y. Feng and H. Li, "Constant Scallop-Height Tool Path Generation for Three-Axis Sculptured Surface Machining," *Computer-Aided Design*, vol. 34, Issue 9, pp. 647-654, Aug. 2002.
- [16] S. Rusinkiewicz and M. Levoy, "Efficient Variants of the ICP Algorithm," in *Proceedings of International Conference on 3-D Digital Imaging and Modeling*, Quebec City, Quebec, Canada, May 28-Jun. 1, 2001.
- [17] F. C. Park and B. J. Martin, "Robot Sensor Calibration: Solving  $AX=XB$  on the Euclidean Group," *IEEE Transactions on Robotics and Automation*, vol. 10, Issue 5, pp. 717-721, Oct. 1994.
- [18] K. Daniilidis, "Hand-Eye Calibration Using Dual Quaternions," *International Journal of Robotics Research*, vol. 18, No.3, pp. 286-298, Oct. 1998.
- [19] N. Andreff, R. Horaud and B. Espiau, "On-line Hand-Eye Calibration," in *Proceedings of International Conference on 3-D Digital Imaging and Modeling*, Ottawa, ON, Canada, Oct. 8, 1999.
- [20] L. X. Hung, V. N. Pi, T. T. Hong, L. H. Ky, V. T. Lien, L. A. Tung and B. T. Long, "Multi-objective Optimization of Dressing Parameters of Internal Cylindrical Grinding for 9CrSi Alloy Steel Using Taguchi Method and Grey Relational Analysis," *Materialstoday: Proceedings*, vol. 18, Part 7, pp. 2257-2264, 2019.